# Preparation and biochemical evaluation of diallyl-thiosulfinate/polyoxyethylene conjugated pH-responsive micelle with enhanced stability, hydrosolubility and antibacterial properties

Souptik Bhattacharya[a], Sayamdipta DasChowdhury[a]

[a] Department of Food Technology, Guru Nanak Institute of Technology, Kolkata, West Bengal, India

*** Corresponding author:** Souptik Bhattacharya

**Email**: souptikjduv@gmail.com; souptik.bhattacharya@gnit.ac.in

**Address:** Department of Food Technology, Guru Nanak Institute of Technology, Sodepur, Kolkata 700114, India.
**Phone:** +91 9831228303
**Orcid id:** 0000-0003-4056-9739

## Graphical abstract

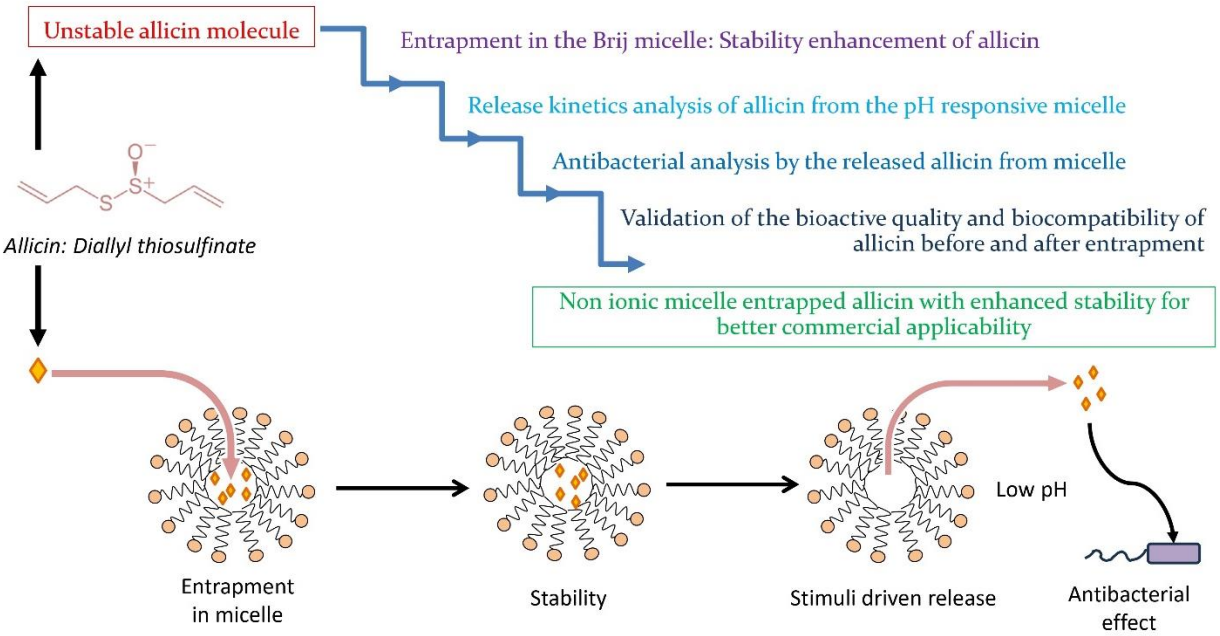

## Abstract

Diallyl-thiosulfinate (allicin) is a major bioactive chemical with several notable therapeutic characteristics of garlic (*Allium sativum*). Nonetheless, one of the biggest concerns regarding the extensive use of allicin in biopharmaceutical commodities is its unstable characteristics. Therefore, utilizing Polyoxyethylene (Brij S20 and Brij 58), appropriate pH-responsive micelle carrier systems have been designed to entrap and improve allicin's stability at an ambient temperature (25 °C) while preserving its quantity and biological activity. Comparing the Brij S20 with the Brij 58 micelle carrier system, the latter demonstrated superior stability and entrapment. In addition, it was found that allicin's stability in micellized condition is significantly influenced by both pH and temperature ($p<0.05$). Additionally, the liberation of allicin from micelle is greatly aided by acidic pH 1.5. The liberation of allicin from the micelle in a controlled manner using lower pH as stimuli may facilitate its biological action at an individual's gastrointestinal lumen or near cancer cell environment having lower pH. Additionally, it was made sure that the micellization method did not impair allicin's bioactivity or reduce appropriate biocompatibility. The current study increases the likelihood of creating a commercially available allicin-loaded, micelle-based formulation for application in biopharma and food related industries.

**Keywords**: Allicin; Brij; Controlled release; Antimicrobial; pH-responsive micelle; Self-assembly;

## Abbreviation

**CMC:** critical micelle concentration; **DLS:** dynamic light scattering; **DSC:** differential scanning calorimetry; **FTIR-ATR:** Fourier transform infrared spectroscopy–attenuated total reflectance; **RS:** radical scavenging; **ADMET:** absorption, distribution, metabolism, excretion, and toxicity; **DT**: Diallyl-thiosulfinate;

## 1. Introduction

Diallyl-thiosulfinate (DT), commonly known as allicin, is the primary organosulfur compound present in garlic (*Allium sativum*) extract. DT possesses a diverse range of therapeutic properties, including anti-inflammatory, anticancer, antimicrobial, rheumatological, wound healing and gastrointestinal (GI) ulcer inhibition properties [1,2]. However, a significant challenge in utilizing DT is its poor stability in aqueous solutions, which hampers its bioavailability [3]. DT functions as a reactive sulfur molecule in the cellular environment of microbes and interacts with thiol-containing proteins via "S-thioallylation". Additionally, it depletes the glutathione pool by reacting with glutathione. Conversely, when DT is metabolized in the human body, it creates hydrogen sulfide, or $H_2S$. As a "gastro-transmitter," this $H_2S$ functions as a chemical messenger in the somatic body, interacting with several physiological and pathological processes [4]. At low concentrations, $H_2S$ functions as a neuromodulator, vasodilator, and inhibitor of proinflammatory molecule production. It also modulates synaptic transmission, improves neuronal excitability and survival, lowers oxidative stress, advocates the secretion of gastric juice and enzymes, and prevents the growth of certain microbes that are non-beneficial to the gut microbiota [4]. Hence, DT has a wide application in the food and nutrition sector, but it is being restricted by its high reactive, unstable and heat labile nature.

Exposure to high $H_2S$ levels can be hazardous for an individual's health. Excessive amount of $H_2S$ has been linked to a few illnesses, including ulcerative colitis, heart problems, and neurological diseases. Therefore, DT's release must be balanced and regulated. Moreover, shortly after it is formed, DT starts to break down and produces a variety of sulphide compounds, including tri-, di-, and cyclic disulfides. DT also reacts with non-polar chemical solvents and in high temperature it produces cyclic disulfides and ajoene [5]. Therefore, a suitable carrier matrix is necessary to deliver ample amount of DT in the body which may increase its bioavailability. Additionally, a controlled release type discharge method is also

needed to steadily supply DT without causing any undesired toxicity due to overdose that may happen because of burst release. Entrapping sensitive molecules in micelles is one method to prevent them from being broken down in the gastrointestinal system [6]. Phytochemical delivery makes extensive use of a variety of biocompatible non-ionic polymers, including long chain fatty acids, polyethylene glycols, poloxamer, alkyl esters, alkyl polyglycerol ethers, sorbitan esters and brij for this purpose [7,8]. Above their critical micelle concentration, these polymers can naturally develop nano-scale assemblies (from 1 to 200 nm) micelles [9]. The 'corona,' an outside hydrophilic shell that affects *in vivo* pharmacokinetics, is attached to a central hydrophobic core in these assemblies. The core is in charge of preserving the solubility, release, entrapment, and stability of the entrapped molecules [10]. The entrapped molecules are protected against deactivation, degradation by the liver and needless breakdown by a variety of *in vivo* stimuli by the core-shell structure of the micelle. *Ergo*, micelles are a potential option for DT's efficient administration because of their capacity for targeted drug release [11].

Due to the low toxicological profile and affordability, Polyoxyethylene (20) cetyl ether (Brij 58: $HO\text{-}(CH_2CH_2O)_n\text{-}(CH_2)_{15}\text{-}CH_3$, n~58) and Polyoxyethylene (20) stearyl ether (Brij S20: $C_{18}H_{37}(OCH_2CH_2)_nOH$, n~20) are often employed as emulsifiers, surfactants, and excipients in a variety of bioformulations [11–13]. Brij is a polymeric, biocompatible, non-ionic surfactant with self-assembly property [14]. Brij molecules have a hydrophilic head and a hydrophobic tail, making them amphiphilic [15]. Above critical micelle concentration (CMC) Brij spontaneously forms micelles [16] that can solubilize substances with low water solubility through hydrophobic interactions/H-bonding because of their lipophilic core and hydrophilic surface [17]. Moreover, micelles produce steric hindrance, which restricts the drug's interaction with the surrounding environment and maintains the entrapped drug's stability over time. Utilizing surfactants, like Brij, is an efficient, quick, and biocompatible method which may improve DT's solubility, stability, and bioavailability [18]. Moreover, polymer-based micelles

provide tailored drug administration by regulating the release profile of the entrapped molecules in response to a particular stimuli like pH or temperature [19]. These traits of micelles can enhance drug penetration, delivery retention and drug accumulation at target sites for improved therapeutic outcomes [20]. From different literatures it was understood that some research on the DT's stability was done previously [21–24]. However, utilization of non-ionic polymer based micellization process to increase the stability of DT at ambient room temperature and study of DT's sustained release profiling from the micellized core is still inadequate. Moreover, a proper toxicological analysis of DT is scarce for promoting its application in commercial biopharmaceutical products.

Therefore, in this research work, an attempt was made to formulate a delivery vehicle system for DT based on Brij (S20 and 58) micelle. The micelle-DT conjugate system increases the DT's shelf life and reduce its spontaneous degradation. Assessments were made of the effects of environmental variables on DT within the micelle, including temperature and pH. Additionally, parametric effects on the drug's release behaviour from the Brij micelle containing DT were examined. However, DT's bioactive potential may be hampered during entrapment by the micellization process and subsequent release of the drug. Hence, various quality parameter tests were conducted before and after DT's release from the produced micelle. For its continued use, it is crucial to determine if the released DT from the micelle retains its bioactive properties. Thus, DT's antibacterial bioactivity was assessed on live bacterial strains following its release. Moreover, DT's ADMET (absorption, distribution, metabolism, excretion, and toxicity) analysis and prediction of probable targets associated with important diseases were done through *in silico* mode to understand its effect on human body after entering through oral route. Moreover, molecular docking and statistical analysis were also done to check the validation of the outcomes.

## 2. Materials and methods

### 2.1. Reagents and strains

Standard DT "(CAS 539-86-6; Purity>98%)" was purchased from "Santa Cruz Biotechnology Pvt. Ltd.". Other necessary chemical and reagents like Brij S20 and 58, Eosin Y dye, concentrated HCl etc. were procured from Merck and "HiMedia Laboratories Pvt. Ltd.". Standard strains of gram-positive and gram-negative bacteria like *Bacillus subtilis* and *Escherichia coli* were procured from NCL, Pune, India and used in this study maintaining proper guidelines as per materials safety datasheet supplied.

### 2.2. CMC point identification of Brij 58 and S20and pH stability analysis of Brij micelles

Water solutions for Brij 58 and Brij S20 (with concentrations ranging from 0.001 to 0.1 mM) were prepared separately at 25 ℃. Eosin Y dye (0.01 mM) was added to each Brij solution as per the standard method of dye micellization technique [25]. A UV-VIS spectrophotometer (Model: JASCO, Japan) was used to measure the samples' absorbance at 540 nm, which represented the absorbance of the dye in the Brij micelles. At 515 nm, the highest absorbance of unattached eosin molecules in liquid was found. The absorbance vs. Brij quantity curve (Figure 1(A) and (B)) was used for the CMC point identification. For the pH stability analysis of the micelles at their individual CMC the absorbance at 540 nm was also checked at pH levels of 1.5, 3, 5, 7, and 9 up to 24 h at 25 ℃. As DT is a heat labile compound higher temperatures were avoided.

### 2.4. DT's entrapment and its shelf-life study in Brij 58 and S20 micelles

1 ml of DT was added in 100 ml water. Then varying amounts of Brij S20 and Brij 58 (0.1-4 mM) was dropwise added (separately) in it with mild stirring. Brij concentrations were gradually raised to their corresponding CMC and higher to induce surfactant's self-assembly and simultaneous trapping of the DT in micelles hydrophobic core. The mixing process took

place for 30 minutes in a light-restricted environment at room temperature (25 ℃) and neutral pH. Then a vacuum lyophilizer (Make: Eyela FDU 1200) was utilized to remove the excess water part. The concentration of DT in micelle was measured periodically for the next 16 days while the samples were kept at room temperature i.e. 25 ºC. As DT is heat labile compound, higher temperature values were not considered for this initial preparation and stability analysis stage. The amount of DT was measured using 4-marcaptopyridine assay method, explicitly mentioned in a previous research work [26]. After 16 days the minimum amount of Brij that stabilized the DT (insignificant amount of degradation than day 2) was noted. That sample was again kept for 2 days at different temperature and pH (20 to 60 ℃ and 3 to 11 pH). After that DT concentration present in the micelle was again evaluated. The % concentration of DT present in the micelle were computed using the following equations [27].

$$Loading\ efficiency\ (\%) = \frac{(Total\ amount\ of\ drug - Free\ amount\ of\ drug)}{Weight\ of\ surfactant\ applied} \times 100 \quad (1)$$

$$Entrapment\ efficiency\ (\%) = \frac{Total\ amount\ of\ drug\ added - Unbound\ drug}{Total\ drug} \times 100 \quad (2)$$

**2.5. Physical description of Brij micelles**

Brij micelle distributed in liquids (1 mg/ml) was taken and their particle size distribution and zeta potential (the amount of the electrical charge at the particle surface) were measured. The Stokes-Einstein equation (Equation 3) for spherical particles was applied to determine the hydrodynamic radius of particles by employing a 633 nm excitation source.

$$D = \frac{kT}{6\pi\eta R} \quad (3)$$

Where, D is diffusion coefficient of the spherical particles residing in a colloidal stage, k is the Boltzmann constant, T is the temperature, η is the medium viscosity and R is the hydrodynamic radius of the particles [17].

The DSC (differential scanning calorimetric) analysis was also carried out for both micellized DT suspension using a Perkin Elmer's DSC 8000 equipment. The samples of interest underwent heating from 10 ºC-90 ºC with 1 ºC/min heating rate. The amount of heat energy required to raise the temperature of the material under investigation (i.e. heat flow) was calculated with respect to temperature. Furthermore, the FTIR spectra was recorded at 25 °C and measured in the range of 500 to 4,000 $cm^{-1}$ by a Bruker Alpha II FTIR-ATR spectrophotometer [16].

### 2.6. Docking analysis

Interactive docking of DT with target compound was done using "SwissDock" web server following standard protocol described elsewhere [28,29].

### 2.7. Determination of the kinetic parameters of DT's release from the micellized core

DT's release study from the micelle was conducted by using a dissolution procedure that has been previously discussed somewhere else with mild modification [27,30]. In short, the pH of the micellized DT solution was reduced to 1.5 (resembling gastric pH) through addition of 0.1M HCl (dissolution medium) in a covered amber glass beaker. The temperature was maintained at 37 ± 0.5 °C, mimicking the body temperature. The amount of liberated DT in the system was determined by sampling at regular intervals. After comparing with different models, the Korsmeyer–Peppas model was found better suitable to explain the release profile [31]. Equation 4 states the model.

$$\frac{N_t}{N_s} = kt^{\alpha} \qquad (4)$$

"Where k is the drug release rate constant. $N_t$ and $N_s$ represent the total cumulative quantity of the released DT at time t and steady state, respectively. 'α' refers to the drug release technique

dependent on the micelle's shape. The 'α' value for a spherical structure system normally varies between 0.43 and 0.85" [32].

### 2.8. *in vitro* antimicrobial quality assessment of the micellized formulations

Actively growing bacterial stock culture in "Mueller Hinton Broth" having around $5.5\times10^7$ living cells were taken (separately for both bacteria species). The simultaneous release of DT from the micelle (by the method described in section 2.7) and the reduction of viable bacterial cell count were observed for both Brij systems. For solid state culture the assessment was performed through inhibition zone measurement using two model bacterial species gram-positive *Bacillus subtilis* and gram-negative *Escherichia coli* [33]. The bacterial stock culture was prepared in a low pH (1.5-2.0) and human body temperature (37 ℃) system so that they can withstand the DT release medium having acidic pH resembling simulated gastric environment which was used to execute the DT's release.

### 2.9. Comparative bioactivity and biocompatibility profile analysis

The standard DPPH ("1-1, Diphenyl-2-picryl hydrazyl") test was used to determine the level of scavenging potential (antioxidant activity) as per the previously published protocol [34]. The *in vitro* toxicity of DT-loaded micelles was assessed using the standard "protein denaturation" assay in contrast to ibuprofen as described previously elsewhere [35]. Further, utilizing a standard haemolysis procedure as previously described elsewhere [36], the hemocompatibility of micellized DT with erythrocytes was evaluated for different samples to assess the biocompatibility [37].

### 2.10. *In silico* analysis of DT's ADMET profile

DT's ADMET profile and probable targets were evaluated by the online web servers such as *ADMETlab* 2.0 (https://admetmesh.scbdd.com) and *Super-PRED*

(https://prediction.charite.de/index.php) respectively which operate through Python based machine learning models [38,39].

### 2.11. Statistical analysis

All statistical analysis were carried out using the Minitab 21 program from Minitab Inc., Pennsylvania, USA. The one-way ANOVA, Tukey test and analysis of relative standard deviation (RSD) was used to test for significant differences. Independent variables were regarded as statistically significant when p-value was found less than 0.05.

## 3. Result and Discussions

### 3.1. Studies on the DT entrapment in Brij micelle

The CMC of Brij S20 and 58 are shown in Figure 1a and 1b. Based on the dye micellization technique, it was approximately 0.0717 mM and 0.0511 mM for Brij S20 and 58, respectively. As previously documented in the literature, micellization results in the entrapment of free eosin molecules within micelles, as indicated by a decrease in the system's eosin concentration at 515 nm. Meanwhile, the development of an eosin-Brij complex, which signifies the formation of micelles, was reflected at 540 nm [40].

Figures 1c and d show that the maturation of micelles is limited when the pH is lowered to an acidic state. At different pH levels, there were clear variations in the micelle production (p-value<0.05). Time was discovered to be an irrelevant (p-value>0.05) parameter, nevertheless. As the target compound (DT) is heat labile a fixed temperature (25 ℃) was considered and effect of higher temperature at this initial assessment was not done. The concentration of $H^+$ in the solution and between the micelles rises when the pH of the system is lowered. Due to the negative charges on the Brij micelle's exterior (Zeta potential: −21.22 and −26.45) the existence of $H^+$ ions cause an ionic firmness to occur on the micelle's external perimeter. As a result, the Van der Waals attracting forces increased in significance and caused the micelles to become unstable. However, a good stabilization and durability was seen in the presence of alkali because of the repulsive force caused by the same charge surrounding the negative-charged micelle surfaces [34]. It can be explained from Figure 2 that DT is stable in the Brij micelle that contains above CMC concentration for a duration of 16 days. In contrast, it was observed that within 24 to 48 hours, both the ‘not entrapped DT’ and the ‘DT in the Brij micelle with sub-CMC concentration’ turned unsustainable and degraded rapidly. As per figure 2, it was noticed that after 16 days, Brij S20 at a minimum concentration of 3.5 mM and Brij 58 at a

minimum concentration of 2.5 mM both preserved approximately 87-89% and 96-98% of the DT respectively. The DT concentration did not significantly drop (RSD<5% and p-value >0.05) from day 2 in these Brij micelle suspension. DT level does not seem to increase by increasing Brij concentration further. Hence, these two concentrations of respective Brij were considered for further studies. In those concentrations of Brij 58 and Brij S20, the drug loading capacities were around 86.36±0.6% and 78.45±0.3%, respectively. Brij 58 and Brij S20 had concurrently showed entrapment efficiencies of 85.81±0.24% and 77.36±0.18%, respectively. From molecular interaction analysis as depicted in Figure 2c (DT as ligand and Brij as target) it was understood DT molecules have affinity towards the hydrophobic region of the Brij micelles. There are three possible pockets in Brij 58 molecule for DT whereas the Brij s20 have one pocket which might be a reason for better outcome exhibited by the Brij 58.

The mean hydrodynamic diameter (d) values for Brij 58 and Brij S20 micelles (8.11 nm and 7.52 nm, respectively) determined by dynamic light scattering (DLS) are shown in Figure 3. The size of Brij 58 and Brij S20 micelles grew with the incorporation of DT to 50.75 nm and 43.82 nm, respectively, indicating efficient trapping of DT within the micelle. Another interesting finding was that the relevance of the negative zeta potential increased with Brij concentration. Generally, similarly charged particles repel each other, preventing agglomeration. As a result, similarly “charged particles” are usually found to be better segregated than “uncharged” ones [41]. The relevance of the “zeta potential” values in this case implies that the DT entrapping micelles are evenly segregated, and have a longer stability, which is the primary explanation for DT's extended presence in the Brij micelle. Deng et al. (2016) and Bhattacharya et al. (2022) made similar observation where biomolecules were effectively preserved by non-ionic micelles [7,41].

### 3.2. Thermal and pH stability analysis of DT in micelle

The effects of pH and temperature on DT-entrapped micelles are depicted in Figure 4a and b. The micelles entrapping DT were found to be stable between 20 and 50 ℃ [36,42]. Furthermore, it was shown that the pH range of 6.5 to 7.2 and 5.6 to 10.0 was optimal for the stability of micelle holding DT for Brij S20 and Brij 58 respectively, as lowering the pH interferes with micelle formation. Lowering the pH causes the concentration of hydronium ions in water to rise, as was mentioned in section 3.1. As a result, the micelles' surface charges become neutral, which is followed by enlargement due to coalescence and, in the end, the micelle formation becomes unstable.

The significant protonation of the polymer's tertiary residues was responsible for the observed abrupt enhancement of the DT-loaded micelles' zeta potential toward positive values (−7.4 mV and −5.4 mV for Brij 58 and Brij S20, respectively) when the pH was lowered [34]. Because the zeta potential values are below the threshold (around −20 mV) for being colloidal, the micelle assembly was compromised [20]. On the other hand, increasing the system temperature causes the micelle to enlarge as a result of water penetration and leaking of the entrapped chemical [43]. As a result, when temperature rises, the amount of DT that is contained inside the micelle significantly drops.

The micellized formulations' differential scanning calorimetry (DSC) thermogram is displayed in Figure 4c. The structured H-bond network between the water molecules and surfactant in the micelle breaks down more readily as the temperature rises. An endothermic peak, which represents the detachment of micelles or the de-micellization process, appears in the DSC curve because of this phenomenon, which disrupts the integrity of the micelles [44]. The de-micellization of DT-Brij micelles was seen above 50ºC, with Brij S20 exhibiting it at 51.6ºC and Brij 58 at 55.8ºC. The Brij 58 micelles are further stable and more heat resistant than the

Brij S20 micelles. The peak's width indicates that the micelle disintegration happens gradually and that the process happens steadily than abruptly [44].

DT in micellized condition has higher concentration in the water since it is only sporadically soluble in it. Conversely, if the micelle formation becomes unstable, DT degrade with time. Figure 5a and b demonstrate how, at temperatures over 50ºC, the average micelle diameter decreased by more than 5 times. It ensures a rise in the amount of free DT in the extract as a result of micelle disintegration [43]. Furthermore, it was noticed that applying a high temperature reduces the micelle structures irreversibly and decreasing the temperature to room temperature i.e. 25°C again thereafter did not change the shape of the DT-loaded micelle. As a result, it was discovered that temperature-induced harm to DT-loaded micelles was permanent. The results of the two-way ANOVA test show that the stability of DT within Brij 58 and S20 micelles is substantially impacted by temperature and pH. They are extremely important regulating variables (p-value <0.01 and F-value > $F_{critical}$). Additionally, the existence of DT in the micelle was established by the FTIR spectra as observed in figure 5c. After entrapment, the peak observed at 1032 $cm^{-1}$ of the FTIR spectra represents the S=O group present in the DT [26].

### 3.3. Analysis of release kinetics of DT from Brij 58 and S20 micelles

Figure 6a shows that DT released from the Brij micelle at pH 1.5 did gradually rather than all at once. For Brij 58 and Brij S20, respectively, more than 71 percent and 58 percent of the loaded medicines were released. Within 300 minutes, the majority of the DT release from Brij S20 micelles was seen. On the other hand, Brij 58 showed about 330 min to reach a steady state. The cumulative release % data were fitted into the Korsmeyer–Peppas model here the $R^2$ values were more than 0.98 in both cases as shown in figure 6b and c. The diffusional exponent, "α" value was derived from the fitted model provides insight into the process of DT release

from Brij micelle. Moreover, most of the points resides within the prediction band and the deviations are very low than the confidence band. The micelle destruction leads to drug release, as evidenced by the α values of 0.52 and 0.50 for DT release from Brij S20 and Brij 58 micelles, respectively. The k values for Brij S20 and Brij 58 were determined to be 1.85 and 1.27 $min^{-1}$, respectively. These values indicate that DT is released from the Brij S20 micelles a little bit faster than Brij 58 micelles. It was observed from the molecular docking that the maximum docking affinity of DT with Brij 58 is less (-1.8 Kcal/mol) than Brij S20 (-2.3 Kcal/mol). Therefore, as strong binding leads to low release, the aforementioned results are justified.

The DLS investigation (figure 5a and b) showed that during this release process, the mean diameter of the DT-entrapped Brij micelles progressively reduced, indicating that DT had been released from the micelle. Robust interaction between drug and micelle frequently encourages delayed drug release. This is advantageous for DT's regulated release [45]. This longer release period may be caused by the larger size of Brij 58 micelle compared to the Brij S20 [46]. An intriguing option for both DT distribution and reducing its degradation is the use of stimuli-responsive Brij micelles loaded with DT. Here, pH acts as a vital stimulus that facilitates the Brij micelles to release the DT from its core by altering the peripheral hydrophilic surface moieties of the Brij micelles [47]. Thus, the produced "DT loaded pH-sensitive micelles" demonstrated superiority in terms of preserving the shelf life of DT and the amount of time needed for its release when compared to several earlier traditional approaches [48].

### 3.4. Antibacterial bioactivity profile of the micellized DT

In accordance with Figure 7a, the dispersion of DT from the Brij micelle plays a crucial role in regulating the suppression of bacterial growth. At the neutral pH (pH 7), a significant reduction in growth was not observed due to the diminished penetration of DT entrapped Brij micelles into the cells of *B. subtilis* and *E. coli*. This reduced penetration can be attributed to the higher

viscosity and 'steric hindrance' instigated by the larger dimensions of the micelles [41]. Additionally, bacteria often have negative potential on their outer walls, ranging from five to thirty mV. Since the DT-entrapped Brij micelle shares similar negative surface charge, micellized DT gets repelled by the bacterial cells. Thus, preventing its entry into the cells and resulting in no growth reduction at pH 7. However, at a low pH (<2), the increased protonation augments ionic firmness across the double layer formation of the micelle by eliminating surface charge. This compaction, driven by increased Van der Waal's affinity force, compromises the stability and development of the micelle arrangement. Consequently, at pH 1.5, a significant inhibition (reflected in decreased viable CFU counts) was observed for both strains, indicating the sustained release of DT from the micelle. This release also suggests enhanced mobility for liberated DT across the bacterial cell membrane/wall due to reduced steric hindrance. The reduction in viable cell numbers in *B. subtilis* was slightly greater than that in *E. coli*, indicating that *B. subtilis* is more vulnerable to DT [35]. Comparatively, Brij 58 micellized DT exhibited a 9-11% greater potential for viable cell reduction than Brij S20 micellized DT, attributed to DT's superior stability within the Brij 58 micelle. Furthermore, two-way ANOVA analysis demonstrated that the suppression of bacterial growth resulting from DT liberation from Brij micelles is highly reliant on Brij concentration and system pH ($p<0.05$ in both cases). At low pH, protonated DT becomes more reactive toward the bacterial protein/enzyme thiol groups that are nucleophilic in nature. Thus, it increases the reactivity despite the enhanced stability of DT at low pH [41].

### 3.5. Comparison of bioactivity and biocompatibility profile throughout the micellization process

From figure 7b it was observed that DT contains a potent ability to inhibit protein denaturation, inhibit bacterial growth on solid media and radical scavenging activity. However, the values decreased significantly in case of DT entrapped micelles but the values again increased after

the release of DT at lower pH from the micellized core. Hence, it can be postulated that DT is the primary contributor of the bioactivity of the micellized formulation in both cases. Without the release of DT the micelles could not inflict the bioactivity properly because the entrapped DT could not get released. However, due to better sensitivity as observed in the liquid media system, *B. subtilis* showed better inhibition zone diameter than *E. coli*. Hence, this substantiates the pH responsive nature of the formulation, where the drug release and its further action can only occur after attaining the favourable stimuli which is low pH in this case. Moreover, none of the formulations exhibited any significant haemolytic activity (<5%) and protein denaturation property and these results validate the non-aggressive nature of the micelle-based formulations. *Ergo*, the serum protein denaturation inhibition experiment demonstrated that the DT-loaded micelles had no substantial adverse or inflammatory effects, owing to their benign characteristics. Hence, from all results it can be said that the DT loaded micelles possess biocompatible profile and retains necessary characteristics to be used as oral formulations.

### 3.6. *in silico* ADMET profile analysis of DT and docking analysis

From the ADMET analysis it was observed that DT is a good candidate for being an orally administrated drug. DT has suitable physicochemical property; all the values fall under the favourable range (Fig. 8). The detailed ADMET profile with explanation and description is given in the supplementary material (*quod vide* Table S1). There was no violations of Lipinski's rule and good intestinal permeability was observed. However, its bioavailability is low due to its unstable nature [22]. Favourable values were observed for somatic distribution, metabolism and excretion. Toxicity profiling revealed that DT is not a significantly toxic compound but it is an irritant for eye and skin. Hence, its entrapment is much needed. Moreover, the dose of DT needs to be optimized before oral use because it may cause stomach discomfort and hepatotoxicity at high dose [1].

The list of predicted targets of DT are given in supplementary file (*quod vide* Table S2). Various targets were observed for DT that includes Neuronal acetylcholine receptor, Vitamin D receptor, Cathepsin D, Neurokinin 2 receptor, Epidermal growth factor receptor erbB1, Adenosine A2b receptor, Cystic fibrosis transmembrane conductance regulator, Histone deacetylase 3 etc. with model accuracy >95%. These proteins are involved in various agonist and antagonist functions in diseases like Alzheimer disease, Acute myeloid leukaemia. Hyperparathyroidism, Osteoporosis, Solid tumour, cancer, Asthma, Chronic obstructive pulmonary disease, Irritable bowel syndrome, Arthritis, Inflammation, Bacterial infection, Rheumatoid arthritis, Head and neck cancer, Gastric adenocarcinoma, Wound healing, Heart failure etc. DT's strong bioactive nature is manifested by its involvement in regulating these proteins or enzymes [4]. However, detailed elucidation of identifying the mode of action of DT on all of these proteins are subjected to future study.

## 4. Conclusion

The current study designed a micelle transporter system based on Brij, a non-ionic surfactant, to encapsulate and stabilize DT. Compared to the solution of only DT, the micellized method improved the stability of the DT to 96-98% by Brij 58 (2.5 mM) and 87-89% by Brij S20 (3.5 mM) for at least 16 days at room temperature 25 ºC. The DLS analysis verified that the trapping of DT led to an increase in the hydrodynamic size of the micelles. Zeta potential readings also demonstrated the colloidal stability of the DT-entrapped micelles. The stability of DT within the micelle was shown to be significantly influenced by the formulation's pH and temperature. Over 50 ºC and in an acidic pH, the micellized system's integrity began to deteriorate. In comparison to the pH-responsive Brij S20 micelle, the pH-responsive Brij 58 micelle displayed extended DT release profile at a slower pace. Nonetheless, in comparison with Brij S20 micelle, Brij 58 micelle demonstrated around 20% superior maximum release with a 31.3% lower release rate confirming a sustained release pattern. Additionally, it was noted that the micelle

did not release DT at neutral pH 7, but in the presence of correct stimuli i.e. acidic pH 1.5, the DT's release was evident and supported by distinct inhibitory zones while utilizing *E. coli* and *B. subtilis* as model strains. The formulation was found biocompatible and exhibited upholding the bioactivity of DT in both type of Brij surfactant. Controlled release with pH regulation can limit unnecessary release of DT during administration through oral route or during systemic circulation by blood, which frequently results in the loss or deterioration of important therapeutic molecules. The fabricated formulation's impact can be maximized by stimulating the release selectively at the intended target location by intestinal or intracellular pH stimulation. This is an essential characteristic for advancing the administration of DT for antibacterial chemotherapy and cancer treatment. It was also shown that two significant limiting variables for the release of DT from the micelle were the presence of appropriate pH level and the concentration of Brij. As a result, the Brij 58 micelle that was created effectively extended the shelf life of DT, generated an DT release profile that was pH sensitive, and showed no appreciable toxicity. Here, pH works as a stimulus to control the release of the DT which can be extremely advantageous for the DT's release in the microenvironment adjacent to the site of tumour or intestinal infections. The produced formulation is intended to be utilized for fortifying various food items.

**Acknowledgements**

The authors would like to thank the department and the institute to carry out the experimental work during the end of COVID-19 pandemic period. The IACS, Kolkata is duly acknowledged for analytical support. The MODROB-REG scheme of AICTE, Government of India, is also acknowledged.

**Declarations of interest**

None

## Reference


[1] S. Xu, Y. Liao, Q. Wang, L. Liu, W. Yang, Current studies and potential future research directions on biological effects and related mechanisms of allicin, Crit. Rev. Food Sci. Nutr. 63 (2023) 7722–7748. https://doi.org/10.1080/10408398.2022.2049691.

[2] E. Catanzaro, D. Canistro, V. Pellicioni, F. Vivarelli, C. Fimognari, Anticancer potential of allicin: A review, Pharmacol. Res. 177 (2022) 106118. https://doi.org/10.1016/j.phrs.2022.106118.

[3] J. Borlinghaus, F. Albrecht, M.C.H. Gruhlke, I.D. Nwachukwu, A.J. Slusarenko, Allicin: chemistry and biological properties., Molecules 19 (2014) 12591–618. https://doi.org/10.3390/molecules190812591.

[4] V.D. Savairam, N.A. Patil, S.R. Borate, M.M. Ghaisas, R. V. Shete, Allicin: A review of its important pharmacological activities, Pharmacol. Res. - Mod. Chinese Med. 8 (2023) 100283. https://doi.org/10.1016/j.prmcm.2023.100283.

[5] D. Ilić, V. Nikolić, M. Stanković, L. Nikolić, L. Stanojević, I. Mladenović-Ranisavljević, A. Šmelcerović, Transformation of Synthetic Allicin: The Influence of Ultrasound, Microwaves, Different Solvents and Temperatures, and the Products Isolation, Sci. World J. 2012 (2012) 1–7. https://doi.org/10.1100/2012/561823.

[6] F. Buyukozturk, J.C. Benneyan, R.L. Carrier, Impact of emulsion-based drug delivery systems on intestinal permeability and drug release kinetics, J. Control. Release 142 (2010) 22–30. https://doi.org/10.1016/j.jconrel.2009.10.005.

[7] L.-L. Deng, M. Taxipalati, F. Que, H. Zhang, Physical characterization and antioxidant activity of thymol solubilized Tween 80 micelles, Sci. Rep. 6 (2016) 38160. https://doi.org/10.1038/srep38160.

[8] L. Shi, J. Zhang, M. Zhao, S. Tang, X. Cheng, W. Zhang, W. Li, X. Liu, H. Peng, Q. Wang, Effects of polyethylene glycol on the surface of nanoparticles for targeted drug delivery, Nanoscale 13 (2021) 10748–10764. https://doi.org/10.1039/d1nr02065j.

[9] D. Lombardo, M.A. Kiselev, S. Magazù, P. Calandra, Amphiphiles Self-Assembly: Basic Concepts and Future Perspectives of Supramolecular Approaches, Adv. Condens. Matter Phys. 2015 (2015) 1–22. https://doi.org/10.1155/2015/151683.

[10] A. Gothwal, I. Khan, U. Gupta, Polymeric Micelles: Recent Advancements in the Delivery of Anticancer Drugs, Pharm. Res. 33 (2016) 18–39. https://doi.org/10.1007/s11095-015-1784-1.

[11] A. Raval, P. Bahadur, A. Raval, Effect of nonionic surfactants in release media on accelerated in-vitro release profile of sirolimus eluting stents with biodegradable polymeric coating, J. Pharm. Anal. 8 (2018) 45–54. https://doi.org/10.1016/j.jpha.2017.06.002.

[12] G. Kaur, S.K. Mehta, Developments of Polysorbate (Tween) based microemulsions: Preclinical drug delivery, toxicity and antimicrobial applications, Int. J. Pharm. 529 (2017) 134–160. https://doi.org/10.1016/j.ijpharm.2017.06.059.

[13] W. Xiong, W. Sang, K.G. Linghu, Z.F. Zhong, W.S. Cheang, J. Li, Y.J. Hu, H. Yu, Y.T. Wang, Dual-functional Brij-S20-modified nanocrystal formulation enhances the intestinal transport and oral bioavailability of berberine, Int. J. Nanomedicine Volume 13 (2018) 3781–3793. https://doi.org/10.2147/IJN.S163763.

[14] S. Borbély, Aggregate Structure in Aqueous Solutions of Brij-35 Nonionic Surfactant Studied by Small-Angle Neutron Scattering, Langmuir 16 (2000) 5540–5545. https://doi.org/10.1021/la991265y.

[15] P. Su, X. Ji, C. Liu, W. Gao, R. Fu, C. Tang, B. Cheng, Brij-58 template synthesis of self-assembled thermostable lamellar crystalline zirconia via a reflux-hydrothermal hybrid method, RSC Adv. 5 (2015) 36467–36471. https://doi.org/10.1039/C5RA05296C.

[16] S. Ghosh, A. Ray, N. Pramanik, Self-assembly of surfactants: An overview on general aspects of amphiphiles., Biophys. Chem. 265 (2020) 106429. https://doi.org/10.1016/j.bpc.2020.106429.

[17] X. Yang, L. Xiang, Y. Dong, Y. Cao, C. Wang, Effect of nonionic surfactant Brij 35 on morphology, cloud point, and pigment stability in Monascus extractive fermentation, J. Sci. Food Agric. 100 (2020) 4521–4530. https://doi.org/10.1002/jsfa.10493.

[18] F. Li, A. Raza, Y.-W. Wang, X.-Q. Xu, G.-H. Chen, Optimization of surfactant-mediated, ultrasonic-assisted extraction of antioxidant polyphenols from rattan tea (Ampelopsis grossedentata) using response surface methodology, Pharmacogn. Mag. 13 (2017) 446. https://doi.org/10.4103/pm.pm_159_16.

[19] A. Mazumder, S. Bhattacharya, C. Bhattacharjee, Role of Nano-photocatalysis in Heavy Metal Detoxification, in: 2020. https://doi.org/10.1007/978-3-030-12619-3_1.

[20] X.X. Zhou, L. Jin, R.Q. Qi, T. Ma, pH-responsive polymeric micelles self-assembled from amphiphilic copolymer modified with lipid used as doxorubicin delivery carriers, R. Soc. Open Sci. 5 (2018) 171654. https://doi.org/10.1098/rsos.171654.

[21] R. Bala, R. Madaan, S. Chauhan, M. Gupta, A.K. Dubey, I. Zahoor, H. Brijesh, D. Calina, J. Sharifi-Rad, Revitalizing allicin for cancer therapy: advances in formulation strategies to enhance bioavailability, stability, and clinical efficacy, Naunyn. Schmiedebergs. Arch. Pharmacol. (2023). https://doi.org/10.1007/s00210-023-02675-3.

[22] Y. Deng, C.-T. Ho, Y. Lan, J. Xiao, M. Lu, Bioavailability, Health Benefits, and Delivery Systems of Allicin: A Review, J. Agric. Food Chem. (2023). https://doi.org/10.1021/acs.jafc.3c05602.

[23] S. Bose, A. Bhattacharjee, C. Huynh, D. Banerjee, Allicin-Loaded Hydroxyapatite: Enhanced Release, Cytocompatibility, and Antibacterial Properties for Bone Tissue Engineering Applications, JOM 74 (2022) 3349–3356. https://doi.org/10.1007/s11837-022-05366-1.

[24] X. Chen, H. Li, W. Xu, K. Huang, B. Zhai, X. He, Self-Assembling Cyclodextrin-Based Nanoparticles Enhance the Cellular Delivery of Hydrophobic Allicin, J. Agric. Food Chem. 68 (2020) 11144–11150. https://doi.org/10.1021/acs.jafc.0c01900.

[25] S. Bhattacharya, D. Sen, C. Bhattacharjee, In vitro antibacterial effect analysis of stabilized PEGylated allicin-containing extract from Allium sativum in conjugation with other antibiotics, Process Biochem. 87 (2019) 221–231. https://doi.org/10.1016/j.procbio.2019.09.025.

[26] S. Bhattacharya, Application of ultrasonication and PEGylation as green extraction technology for yield intensification of diallyl thiosulfinate (allicin), Process Biochem. 130 (2023) 300–309. https://doi.org/10.1016/j.procbio.2023.04.015.

[27] A. Tomšik, L. Šarić, S. Bertoni, M. Protti, B. Albertini, L. Mercolini, N. Passerini, Encapsulations of wild garlic (Allium ursinum L.) extract using spray congealing technology, Food Res. Int. 119 (2019) 941–950. https://doi.org/10.1016/j.foodres.2018.10.081.

[28] M. Bugnon, U.F. Röhrig, M. Goullieux, M.A.S. Perez, A. Daina, O. Michielin, V. Zoete, SwissDock 2024: major enhancements for small-molecule docking with Attracting Cavities and AutoDock Vina, Nucleic Acids Res. (2024).

https://doi.org/10.1093/nar/gkae300.

[29] S. Bhattacharya, D. Sen, C. Bhattacharjee, Inhibition mechanism study for diallyl thiosulfinate (allicin) against crucial bacterial proteins through in silico molecular docking simulation, Process Biochem. (2022). https://doi.org/10.1016/j.procbio.2022.09.026.

[30] K. Shahani, J. Panyam, Highly Loaded, Sustained-Release Microparticles of Curcumin for Chemoprevention, J. Pharm. Sci. 100 (2011) 2599–2609. https://doi.org/10.1002/jps.22475.

[31] L. Tao, J.W. Chan, K.E. Uhrich, Drug loading and release kinetics in polymeric micelles: Comparing dynamic versus unimolecular sugar-based micelles for controlled release, J. Bioact. Compat. Polym. 31 (2016) 227–241. https://doi.org/10.1177/0883911515609814.

[32] I.Y. Wu, S. Bala, N. Škalko-Basnet, M.P. di Cagno, Interpreting non-linear drug diffusion data: Utilizing Korsmeyer-Peppas model to study drug release from liposomes, Eur. J. Pharm. Sci. 138 (2019) 105026. https://doi.org/10.1016/j.ejps.2019.105026.

[33] M. Balouiri, M. Sadiki, S.K. Ibnsouda, Methods for in vitro evaluating antimicrobial activity: A review, J. Pharm. Anal. 6 (2016) 71–79. https://doi.org/10.1016/j.jpha.2015.11.005.

[34] J. Liao, H. Peng, C. Liu, D. Li, Y. Yin, B. Lu, H. Zheng, Q. Wang, Dual pH-responsive-charge-reversal micelle platform for enhanced anticancer therapy, Mater. Sci. Eng. C 118 (2021) 111527. https://doi.org/10.1016/j.msec.2020.111527.

[35] S. Bhattacharya, P. Chakraborty, D. Sen, C. Bhattacharjee, Kinetics of bactericidal potency with synergistic combination of allicin and selected antibiotics, J. Biosci.

Bioeng. (2022). https://doi.org/10.1016/j.jbiosc.2022.02.007.

[36] H. Fujisawa, K. Suma, K. Origuchi, H. Kumagai, T. Seki, T. Ariga, Biological and Chemical Stability of Garlic-Derived Allicin, J. Agric. Food Chem. 56 (2008) 4229–4235. https://doi.org/10.1021/jf8000907.

[37] P.S. Baviskar, H.S. Mahajan, S.M. Chandankar, Y.O. Agrawal, Development and evaluation of N-acetyl glucosamine-decorated vitamin-E-based micelles incorporating resveratrol for cancer therapy, J. Drug Deliv. Sci. Technol. 78 (2022) 103965. https://doi.org/10.1016/j.jddst.2022.103965.

[38] G. Xiong, Z. Wu, J. Yi, L. Fu, Z. Yang, C. Hsieh, M. Yin, X. Zeng, C. Wu, A. Lu, X. Chen, T. Hou, D. Cao, ADMETlab 2.0: an integrated online platform for accurate and comprehensive predictions of ADMET properties, Nucleic Acids Res. 49 (2021) W5–W14. https://doi.org/10.1093/nar/gkab255.

[39] J. Nickel, B.-O. Gohlke, J. Erehman, P. Banerjee, W.W. Rong, A. Goede, M. Dunkel, R. Preissner, SuperPred: update on drug classification and target prediction, Nucleic Acids Res. 42 (2014) W26–W31. https://doi.org/10.1093/nar/gku477.

[40] A. Patist, J.R. Kanicky, P.K. Shukla, D.O. Shah, Importance of Micellar Kinetics in Relation to Technological Processes, J. Colloid Interface Sci. 245 (2002) 1–15. https://doi.org/10.1006/jcis.2001.7955.

[41] S. Bhattacharya, D. Sen, C. Bhattacharjee, Strategic development to stabilize bioactive diallyl thiosulfinate by pH responsive non ionic micelle carrier system, Process Biochem. (2022). https://doi.org/10.1016/j.procbio.2022.05.027.

[42] H. Wang, X. Li, X. Liu, D. Shen, Y. Qiu, X. Zhang, J. Song, Influence of pH, concentration and light on stability of allicin in garlic ( *Allium sativum* L.) aqueous

extract as measured by UPLC, J. Sci. Food Agric. 95 (2015) 1838–1844. https://doi.org/10.1002/jsfa.6884.

[43] A.K. Sahu, J. Mishra, A.K. Mishra, Introducing Tween-curcumin niosomes: preparation, characterization and microenvironment study, Soft Matter 16 (2020) 1779–1791. https://doi.org/10.1039/C9SM02416F.

[44] S. Sarkar, S. De, Brij Niosomes as Carriers for Sustained Drug Delivery─A Fluorescence-Based Approach to Probe the Niosomal Microenvironment, Langmuir 38 (2022) 4521–4537. https://doi.org/10.1021/acs.langmuir.1c02996.

[45] S. Bhattacharya, D. Gupta, D. Sen, C. Bhattacharjee, Development of Micellized Antimicrobial Thiosulfinate: A Contemporary Way of Drug Stability Enhancement, in: Lect. Notes Bioeng., 2021. https://doi.org/10.1007/978-981-15-7409-2_8.

[46] Z. Xu, P. Xue, Y.-E. Gao, S. Liu, X. Shi, M. Hou, Y. Kang, pH-responsive polymeric micelles based on poly(ethyleneglycol)-b-poly(2-(diisopropylamino) ethyl methacrylate) block copolymer for enhanced intracellular release of anticancer drugs, J. Colloid Interface Sci. 490 (2017) 511–519. https://doi.org/10.1016/j.jcis.2016.11.091.

[47] Y. Liu, W. Wang, J. Yang, C. Zhou, J. Sun, pH-sensitive polymeric micelles triggered drug release for extracellular and intracellular drug targeting delivery, Asian J. Pharm. Sci. 8 (2013) 159–167. https://doi.org/10.1016/j.ajps.2013.07.021.

[48] P. Saveyn, E. Cocquyt, W. Zhu, D. Sinnaeve, K. Haustraete, J.C. Martins, P. Van der Meeren, Solubilization of flurbiprofen within non-ionic Tween 20 surfactant micelles: a 19F and 1H NMR study, Phys. Chem. Chem. Phys. 11 (2009) 5462. https://doi.org/10.1039/b822327k.

**Figure Captions:**

**Fig 1** CMC determination of Brij S20 (a) and 58 (b). Stability of Brij S20 (c) and 58 (d) micelles with time at different pH (p-value less than 0.05 was considered significant).

**Fig 2** Variation in the residual DT percentage with time for varying concentration of (a) Brij 58 and (b) Brij S20 (All the experiments are replicated thrice; error bar showing standard deviation of the mean). (c) Localization of DT molecules on the hydrophobic region of Brij molecules.

**Fig 3** Histograms showing the average hydrodynamic diameter or 'd' of only Brij S20 (a) and Brij 58 (b) micelles. (c) and (d) represents DT entrapped micelles with higher diameter.

**Fig 4** The effect of temperature and pH on DT loaded Brij 58 (a) and Brij S20 (b) micelles. The differential scanning calorimetry (DSC) thermogram of the micellized formulations (c).

**Fig 5** Histograms of the temperature dependent DLS study of Brij S20 (a) and Brij 58 (b). FTIR analysis of micellized solution with DT loaded and empty micelle (c).

**Fig 6** Release kinetics analysis and model fitting of the release of DT from the Brij micelles.

**Fig 7** (a) Antibacterial effect of released DT on the living bacterial cells in liquid media. (b) Biocompatibility and quality assay of DT loaded micelles at different steps of micellization process.

**Fig 8** Physicochemical property of DT.

**Fig. 1**

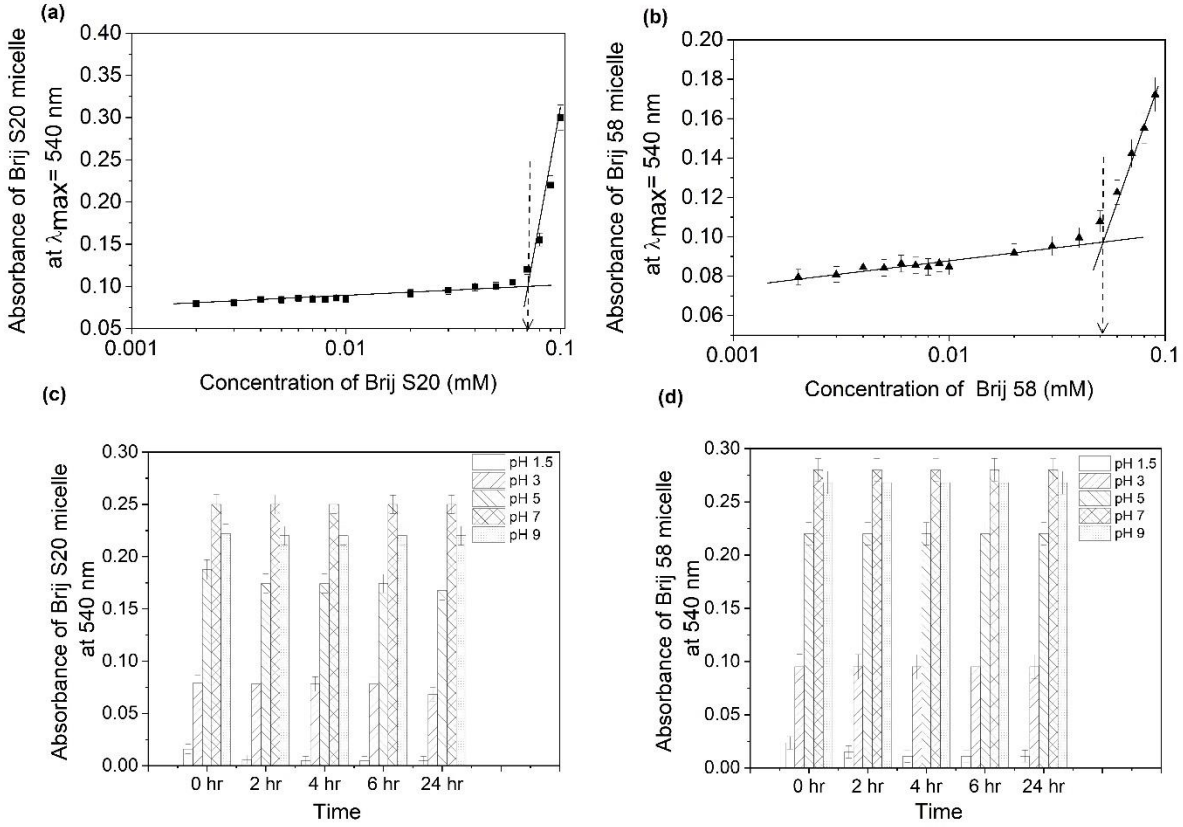

**Fig 2**

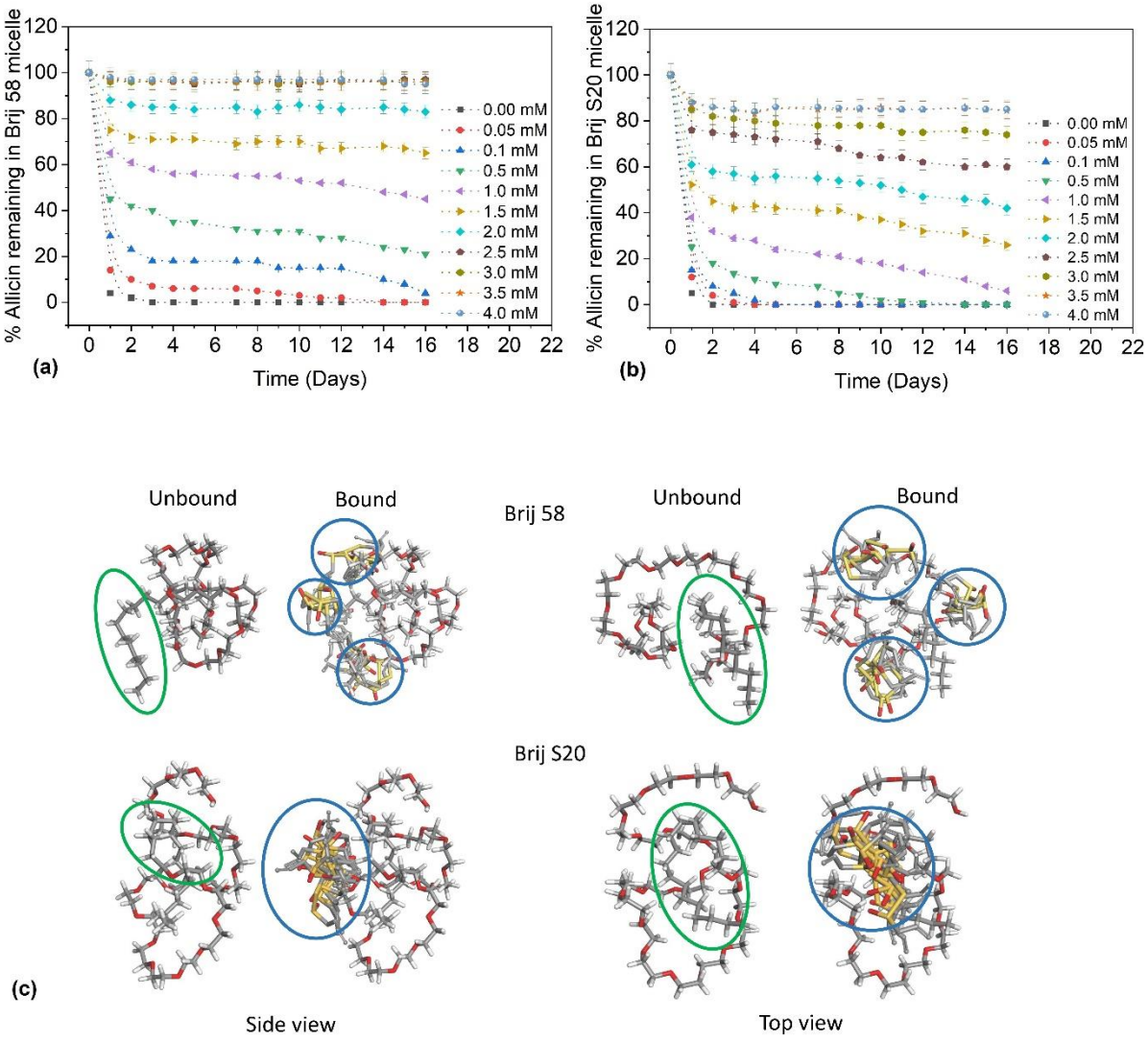

**Fig 3**

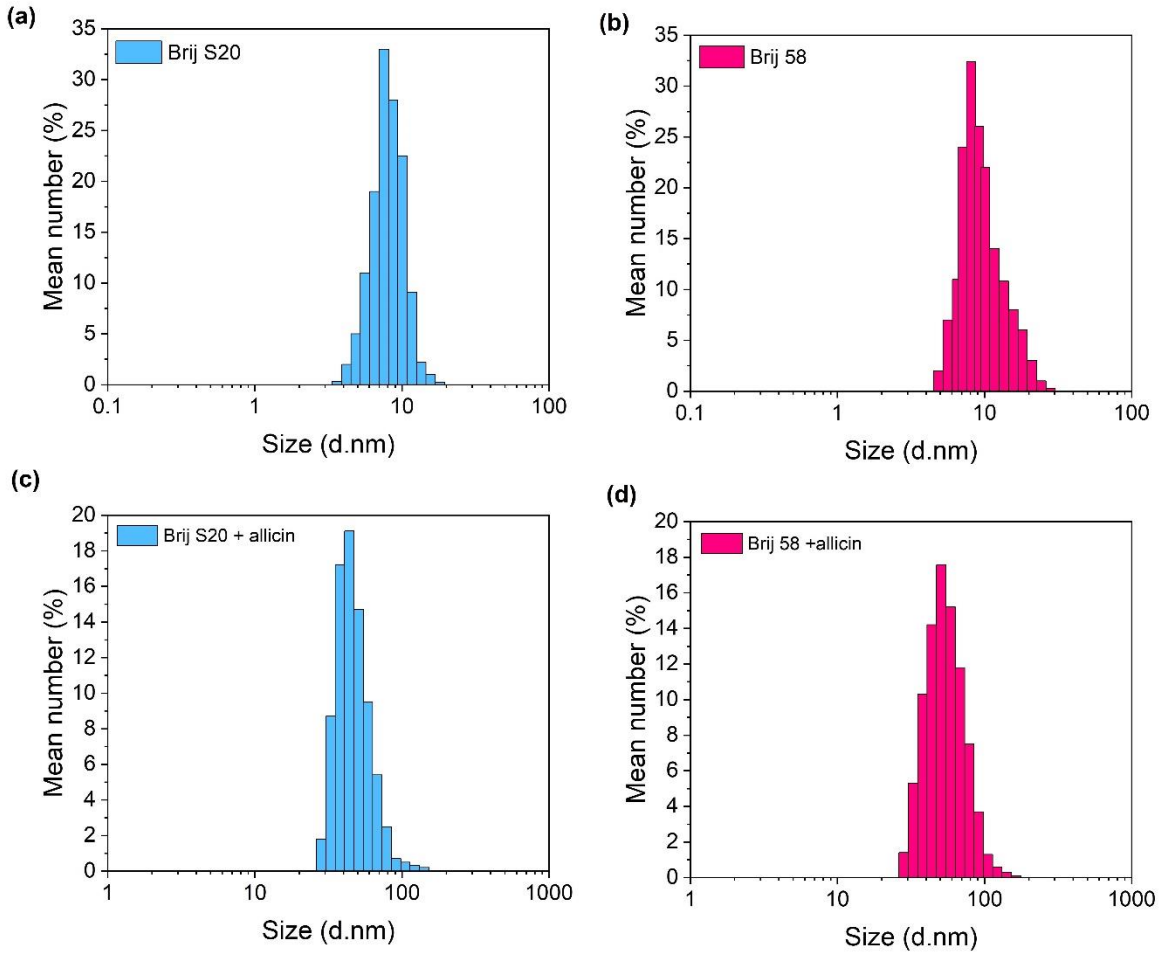

**Fig 4**

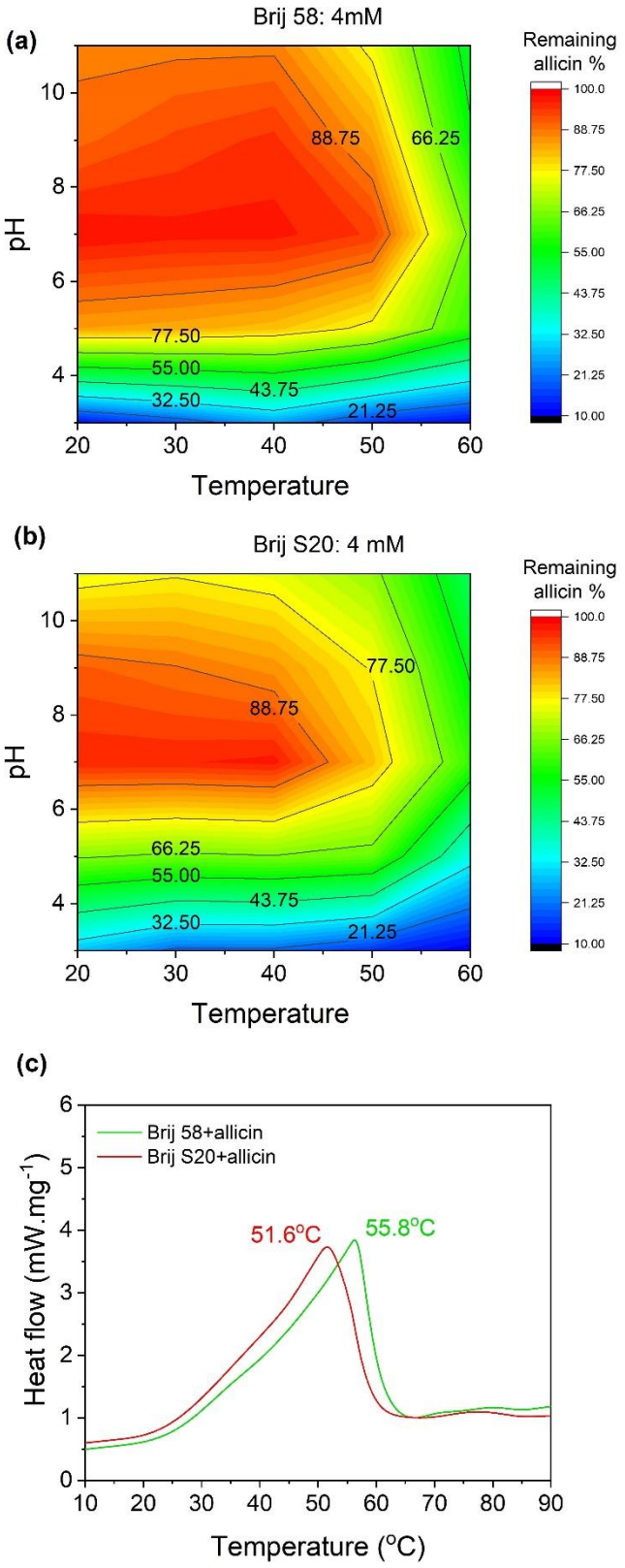

**Fig 5**

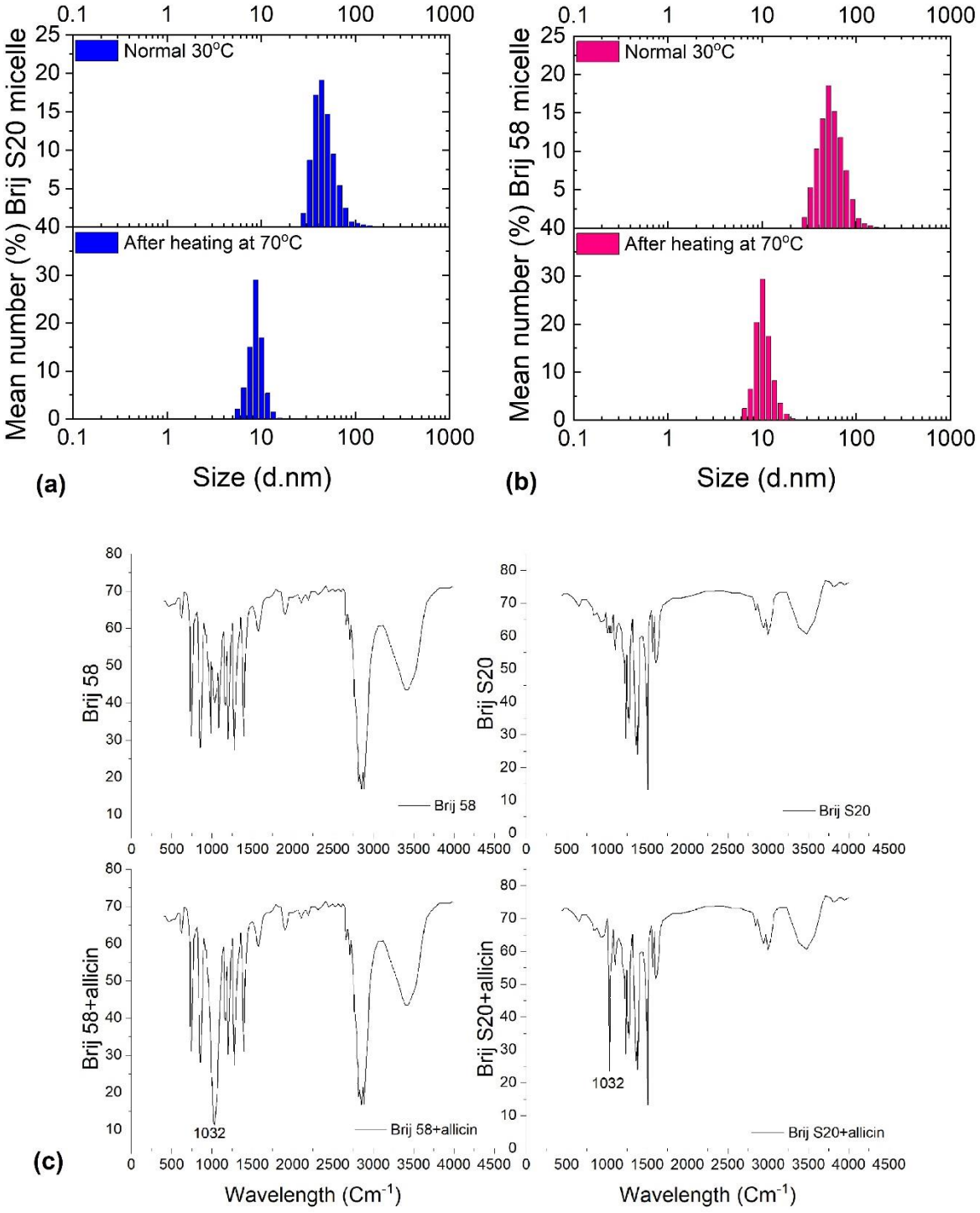

**Fig 6**

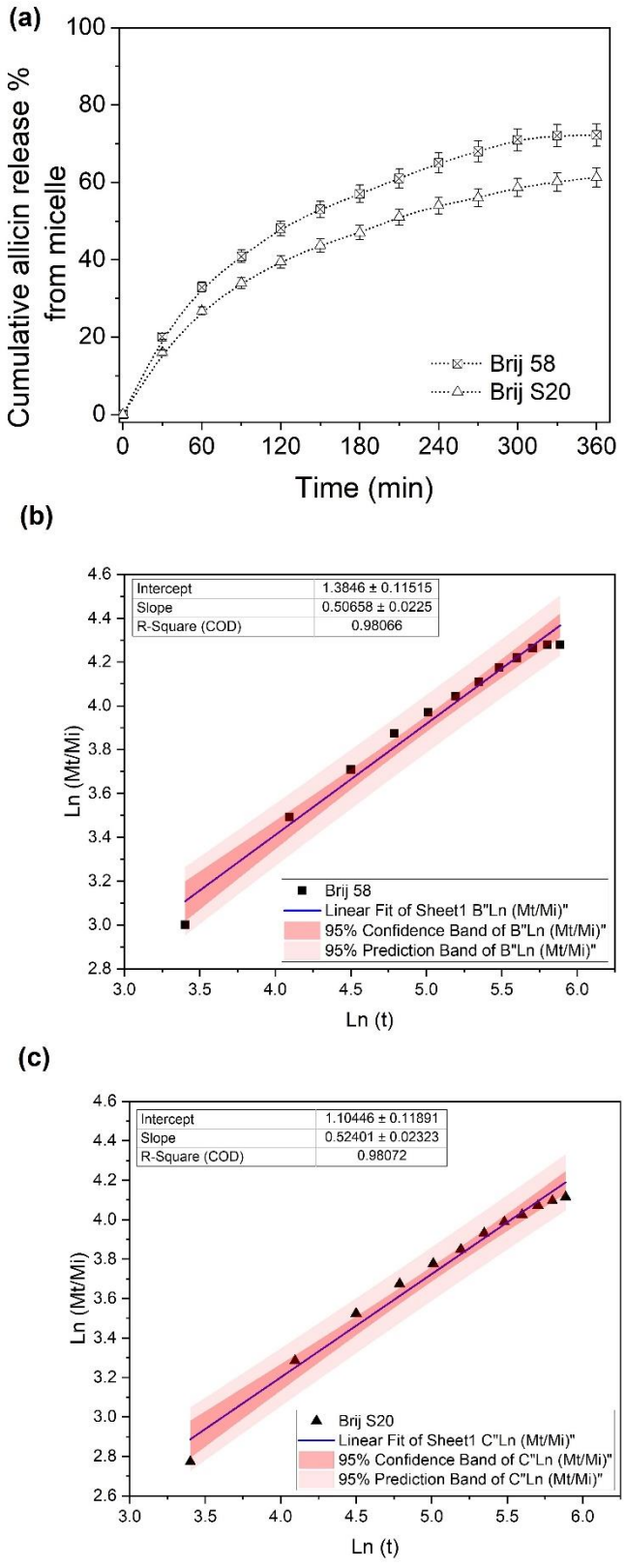

# Fig 7

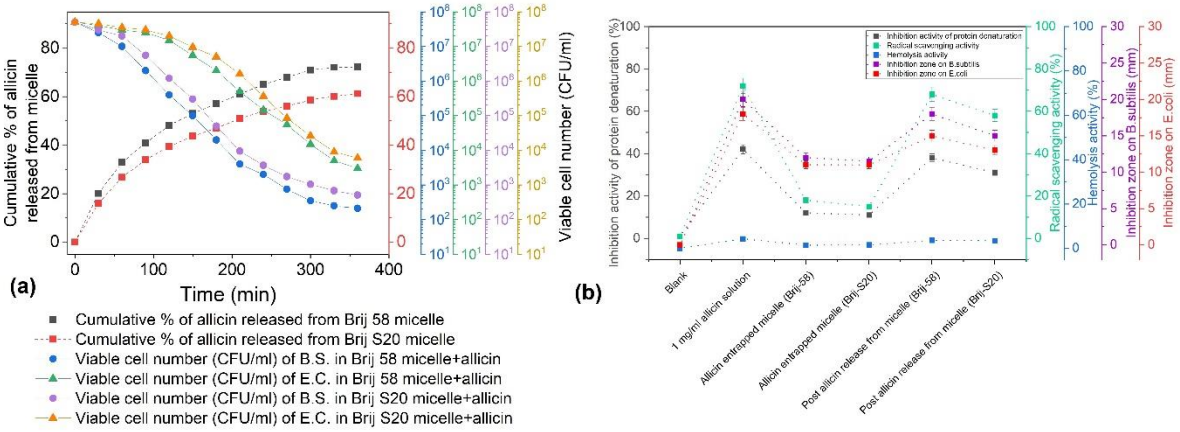

**Fig 8**